

## Factor affecting morphology, thermal and structural properties of pennisetin microparticles prepared by solvent phase separation

A. Bensalem<sup>1,2</sup>, S. Mosbahi<sup>1</sup>, H. Amoura<sup>1</sup>, A. Charabi<sup>1</sup>, M. Rogalski<sup>3</sup>, P. Magri<sup>3</sup>, B. Nadjemi<sup>4</sup>, H. Mokrane<sup>1,\*</sup>

<sup>1</sup>Laboratoire des produits bioactifs et de la valorisation de la biomasse (LPBVB) Ecole Normale Supérieure, B.P. 92, 16050 Vieux-Kouba, Algiers-Algeria.

<sup>2</sup>Département de chimie, Académie militaire de Cherrhell Houari Boumediene, Tipaza-Algeria

<sup>3</sup>Laboratoire de chimie et physique Approche Multi-Echelles des Milieux Complexes (LCP-A2MC) Université de Lorraine, 1 Boulevard Arago, 57078 Metz-France

<sup>4</sup>Laboratoire d'études et de développement des techniques d'épuration, et de traitement des eaux et gestion environnementale (LEDTEG) Ecole Normale Supérieure, BP 92, Kouba, Algiers-Algeria

\*Corresponding author: hind.mokrane@g.ens-kouba.dz / mokrane2017@gmail.com; Tel.:+213555253835;

### ARTICLE INFO

#### Article History :

Received : 01/01/2021

Accepted : 24/05/2021

#### Key Words:

Pennisetin;  
Microparticle;  
Microscopy;  
Thermal properties;  
Fourier transform infrared.

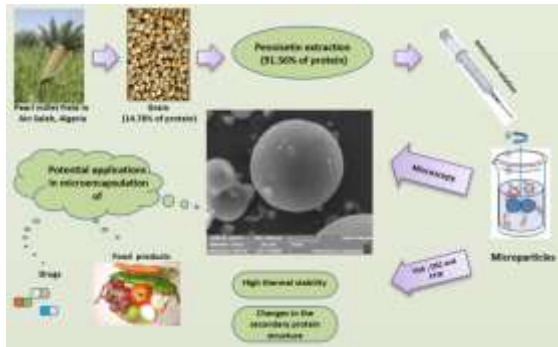
### ABSTRACT/RESUME

**Abstract:** Pearl millet prolamin, a non gluten protein called pennisetin, was used to formulate microparticles by phase separation, using glacial acetic acid (10%) and aqueous ethanol (70%). Optical microscopy (OM) and scanning electron microscopy (SEM) showed that microparticles produced by aqueous ethanol (ME) were spherical with smooth surface and their average diameter was  $13 \pm 2 \mu\text{m}$ , whereas those prepared with glacial acetic acid (MA) were irregularly shaped with tough surface and high diameters ranging from 22.87 to 119.25  $\mu\text{m}$ . ME morphology was highly affected by antisolvent concentration and mixing speed. Thermogravimetric analysis (TGA) indicated that microparticles began losing weight at 60°C probably due to water evaporation, then a second step of degradation occurred at higher temperature 318, 324°C and 308°C for ME, MA and pennisetin powder, respectively. The differential scanning calorimetry (DSC) showed that ME were more heat stable than MA and the original pennisetin powder. Fourier transform infrared (FTIR) spectra showed an increasing formation of  $\beta$ -sheet structure in ME and MA indicating tendency to protein aggregation during microparticle formation. The pennisetin microparticles developed in this study could be used in bioactive compounds encapsulation for vegans and celiacs.

### I. Introduction

Microparticles are known as small size particles ranging between 1 to 1000  $\mu\text{m}$  containing active agent surrounded by synthetic or natural biodegradable membrane [1]. Microparticles are composed of two parts, namely the core and the shell. The core (the internal part) contains the active agent, while the shell (the external part) protects the core from the outer environment [2]. In recent

years, the utilization of vegetable proteins as shell material especially in food and drug encapsulation increased [2-4]. This is probably due to their renewable and biodegradable character, in addition to their good acceptance by religious and vegetarian communities, in contrast to animal proteins such as casein [5], bovine serum albumin and lysozyme [6] and gelatin [7].



Graphical abstract

Prolamins are hydrophobic proteins constituting the major storage fraction in most cereal seeds. Specific names have been given for each cereal prolamin. Thus, zein, hordein, gliadin, kafirin and pennisetin are known as prolamin of corn, barley, wheat, sorghum and pearl millet, respectively [8, 9]. Pennisetin has been detected in three forms with respectively molecular masses of 27, 22 and 12 kDa-pennisetin [10]. Pennisetin is a non gluten protein which made it suitable for population suffering from celiac disease. Compared to other cereals, greater quantity of pearl millet grains could be produced in short growing season and under harsh conditions such scanty rain fall, infertile soil and intense heat [8, 10].

In the two past decades, prolamin microparticles received much more interest in research, due to their important functional properties and potential food applications [11, 12]. In this context, gliadin microparticles produced by simple coacervation, were used to encapsulate hexadecane [11]. The effect of gliadin microparticles preparation parameters such as speed and time of mixing were recently investigated [13]. Zein microparticles were used as coating material to encapsulate tomato oleoresin [14], retinol [15] and essential oils [16]. Zein microparticles were also used to encapsulate specific drugs such as Hydrocortisone and Mesalazine [17]. Furthermore, kafirin microparticles were prepared for phytochemicals encapsulation such as phenolic antioxidants [18]. To inhibit digestive amylases in the small intestine, kafirin was also used as a simple delivery system of sorghum condensed tannins [19]. In another work, Prednisolone was successfully loaded into microparticles formulated using kafirin [20]. The use of glacial acetic acid and other organic acids as solvent resulted into the formation of kafirin microparticles by phase separation with many internal holes or vacuoles [21]. Recently, the major protein fraction of proso millet was used as novel curcumin delivery system [22]. But to date and to the best of our knowledge, no study has aimed to produce microparticle from pearl millet pennisetin. Against this background, pearl millet pennisetin was used to prepare microparticles by phase separation. The effect of process preparation:

solvent, antisolvent concentration and mixing speed was studied. Two solvents were used: Aqueous ethanol (70%) and glacial acetic acid (10%). Therefore, the aim of this study was to investigate the pennisetin microparticles morphology by optical microscopy (OM) and scanning electron microscopy (SEM) and to study their thermal stability by thermogravimetric analysis (TGA) and differential scanning calorimetry (DSC). Pennisetin chemical structural changes before and after microparticle formation were assessed by Fourier transform infrared spectroscopy (FTIR).

## II. Materials and methods

### II.1. Materials

Pearl millet sample was harvested from local cultivars commonly called “Bechna beldia” in the arid Sahara areas of south Algeria (In Salah). Pearl millet grains were ground into flour in cyclotec 1093 sample mill (Tecator, Hogånäs, Sweden). The obtained flour was manually sieved over a 500  $\mu\text{m}$  sieve. All chemicals were of analytical grade and were purchased from Sigma-Aldrich.

### II.2. Protein content

The protein content of pennisetin powder and the formulated microparticles ME and MA, was determined using Kjeldahl approved method 46-30 with 6.25 as conversion factor [23].

### II.3. Pennisetin extraction methods

Pennisetin extraction was carried out from dried pearl millet grain flour using a combined and modified methods previously described by Gómez-Martínez *et al.* [24] and Kumar *et al.* [25]. Pennisetin was first extracted with 70% (v/v) aqueous ethanol containing 0.1% (w/v) sodium hydroxide and 0.1% (w/v) sodium metabisulfite at 50 °C for 1 h with continuous stirring (900 rpm). Then, at room temperature and under continuous stirring (400 rpm), pennisetin was precipitated by diluting the extract with demineralized water to bring ethanol concentration below 20% (v/v). The pH was then adjusted to the pennisetin isoelectrical point which is between 4.0-4.5 with hydrochloric acid HCl (1 M) and sodium hydroxide NaOH (1 M). Iterative precipitations of the pennisetin were carried out 3 times by solubilizing the precipitated pennisetin in 70% (v/v) aqueous ethanol solution and reprecipitating it by dilution as mentioned above. The obtained wet cake of pennisetin was recovered by centrifugation at 12,000 $\times$ g for 15 min and dried in a hood at 30°C for 12 h. Pennisetin was then defatted using 10 volumes of n-hexane at room temperature.

### II.4. Pennisetin microparticles preparation

Pennisetin microparticles (ME and MA) were respectively prepared by aqueous ethanol or glacial

acetic acid. In order to form homogeneous particle size and high percentage of microparticles, the effect of stirring speed and concentration of antisolvent solution on microparticle diameter and formation were assessed.

The best preparation conditions were described below. Under continuous stirring (600 rpm), 0.2 g of pennisetin was respectively dissolved in 10 g of 70% (v/v) aqueous ethanol at 50°C to prepare ME or in 10 g of 10% (w/w) glacial acetic acid at room temperature to prepare MA. The two solutions were allowed to rest for 16 h on cooling at room temperature to improve pennisetin precipitation. The suspension was then heated at 30°C to dissolve the pennisetin. The antisolvent solution 1.0% (w/v) of sodium chloride was added at ambient temperature during 5 min under continuous magnetic stirring to reach total weight of 20 g. Stirring and temperature were maintained for 5 min after this operation. During addition of antisolvent, microparticles were formed. After ME and MA formulation, the ethanol and glacial acetic acid were removed by centrifugation and the pellet of microparticles was washed three times with distilled water. The supernatant was then removed by drying the pellet of microparticles at room temperature.

## II.5. Microparticles characterization

### II.5.1. Optical microscopy

The ME and MA microparticle diameters were measured at room temperature from optical microscope images (AXIOSKOP 40, ZEISS, Germany). Diameter measurements were made using Axio-Vision microscopy software for image analysis.

### II.5.2. Scanning electron microscopy (SEM)

The morphology of pennisetin microparticles was observed using a field emission scanning electron microscope (FE-SEM) (JEOL J7600F, Germany). The SEM images were acquired with a fixed electron beam at low accelerating voltage (20 kV). Diameters and morphology of the pennisetin microparticles were determined from SEM images.

### II.5.3. Thermogravimetric analysis (TGA)

Thermal balance 2050 TGA V5.4A (TA instruments, USA) was used to study the thermal decomposition of pennisetin powder and the microparticles MA and ME. The characteristic feature of this equipment was that the heating rate was coupled with the mass loss. Therefore, the sample temperature was kept constant until the mass loss, corresponding to a completed chemical

reaction. The thermal evolution of the raw materials was followed from the room temperature up to 450°C with a gradual increase of 10°C per minute. The average mass of the sample used, was of about 5 mg.

### II.5.4. Differential scanning calorimetry (DSC)

Differential scanning calorimetry (DSC) analysis of 5 mg of pennisetin powder, MA or ME samples was carried out using a differential scanning calorimeter DSC-8500PC (Netzsch, Germany) at a heating rate of 5°C/min from room temperature to 300°C under nitrogen atmosphere using a flow rate of 50 mL/min. The samples were placed in sealed aluminum pans and a sealed empty pan was used as reference.

### II.5.5. Fourier transform infrared spectroscopy (FTIR)

The dried pennisetin microparticles (ME and MA) and pennisetin powder were characterized by diffuse reflectance-FTIR (DRIFT). FTIR spectra were obtained on a Perkin Elmer spectrometer (Spectrum One FTIR, USA), operating in the region from 4000 to 650 $\text{cm}^{-1}$  with 4 $\text{cm}^{-1}$  of resolution. All the results were normalized and the content of protein secondary structures were evaluated using peakfit software V4.12. Second derivative function of the amide I region situated between 1600 and 1700  $\text{cm}^{-1}$ , was then carried out using a smoothing point of 20%. The pennisetin and microparticles secondary structure in the amide I region were obtained as percentage of amide I total area from the Gaussian curve fitted bands. The changes in the pennisetin secondary structure during microparticles formation were evaluated by the ratios of  $\alpha$ -helix to  $\beta$ -sheet and amide I to amide II.

### II.6. Statistical analysis

Analyze of variance of antisolvent concentration and mixing speed was achieved using Tukey's multiple comparison procedure on a 5% significance level. Statistical study was performed using the Statistical Analysis System R 4.0.2. [26]. All measurement were repeated at least three times and expressed as mean  $\pm$  standard deviation.

## III. Results and discussion

### III.1. Protein Content

Total protein content in the Algerian pearl millet grain flour was 14.78% on dry matter (d.m) basis with moisture content of 9.94%. The extracted pearl millet prolamin fraction namely pennisetin showed higher purity compared to previous reports [10],

with protein contents of 91.56% on d.m basis and 5.37% of moisture.

**III.2. Pennisetin microparticle morphology and size**

In food or non-food applications, particle size and shape are paramount parameters to prepare stable microparticles. In the following, the effect of solvent, antisolvent concentration and mixing speed on microparticle morphology was assessed and the observed diameter and shape are shown in Table 1.

**III.2.1. Effect of solvent**

Figure 1 shows the OM images of pennisetin microparticles ME and MA prepared with aqueous ethanol (Figure 1A to 1E) or glacial acetic acid (Figure 1F). Glacial acetic acid allowed MA preparation without adding any antisolvent solution, however, the microparticles were characterized by irregular shape and high diameter varying from 22.87 to 119.25 μm (Table 1). Moreover, MA were more fragile and less stable than ME. Their irregular shape probably resulted from the aggregated fragments which form bigger microparticles. Whereas, the formation of ME emulsions required adding sodium chloride as antisolvent (Figure 1A to 1E). The pennisetin microparticle morphology was highly affected by type of solvent. ME appeared more regular and homogeneous than MA. Thus, the effect of antisolvent concentration and mixing speed was investigated.

**III.2.2. Effect of antisolvent solution concentration**

Variable shape and size of ME were obtained from irregular to spherical when varying antisolvent concentration (Table 1). Figure 1A to 1E show the OM images of ME prepared with increasing percentage of sodium chloride in antisolvent solution. The required spherical and regular microparticle shape was obtained at lower sodium chloride concentration 1 and 2%. At higher antisolvent concentration, the microparticles tend to aggregate and to disappear. The antisolvent concentration significantly affected ( $p < 0.001$ ) ME size and shape.

**III.2.3. Effect of mixing speed**

The effect of mixing speed on ME diameter and shape is shown in table 1. A highly significantly difference ( $p < 0.001$ ) was found on the effect of the mixing speed on microparticle formation. At all mixing speed, ME are formed and their diameters ranged from 5.20 to 134.35 μm. However, at high mixing speed 400 and 600 rpm, ME diameters ranged from 5.20 to 35.06 μm, the microparticles were homogeneous with spherical shape. The smallest and more regular particle size was obtained with aqueous ethanol at 600 rpm and 1% of sodium chloride with a microparticle diameter range of 5.20 to 15.04 μm and an average diameter of  $13.08 \pm 2.00 \mu\text{m}$  (Table 1).

*Table 1. Effect of antisolvent concentration and mixing speed on the pennisetin microparticles diameter and shape.*

Process parameter		NaCl (%)	Particle diameter Range [min-max] (μm)	Average ± sdev (μm)	Shape (morphology)
Ethanol	Antisolvent concentration solution ***	0		No particle formation	-
		1	11.75 - 35.06	22.79 ± 4.91 <sup>a</sup>	Spherical
		2	12.73 - 99.71	50.07 ± 21.04 <sup>c</sup>	Spherical
		4	7.83 - 87.23	33.98 ± 17.60 <sup>b</sup>	Irregular
		6	11.63 - 86.49	36.66 ± 16.11 <sup>b</sup>	Irregular
		8	17.45 - 132.23	65.61 ± 23.80 <sup>d</sup>	Irregular
	Mixing speed (rpm) ***	100	24.99 - 134.35	56.35 ± 22.55 <sup>D</sup>	Irregular
		150	23.01 - 91.35	62.16 ± 12.57 <sup>D</sup>	Irregular
		200	10.71 - 67.32	31.68 ± 13.56 <sup>C</sup>	Irregular
		400	11.75 - 35.06	22.79 ± 4.91 <sup>B</sup>	Spherical
	600	5.20 - 15.04	13.08 ± 2.00 <sup>A</sup>	Spherical	
Glacial acetic acid***		0	22.87 - 119.25	67.97 ± 28.89	Irregular

Values with different letter in the same column was significantly different ( $p < 0.05$ ). \*\*\* $p \leq 0.001$ , \*\* $p \leq 0.01$ , \* $p \leq 0.05$ .



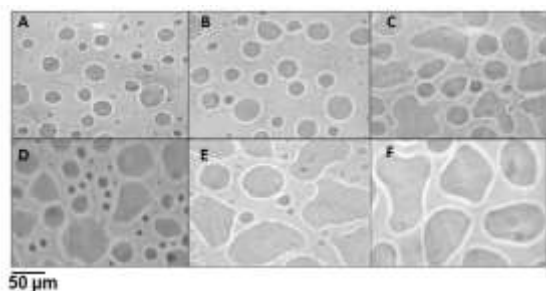


**Figure 1.** Optical microscopy (OM) images of pennisetin microparticles prepared in aqueous ethanol (ME). Effect of sodium chloride concentration on microparticle formation. (A) 1%; (B) 2%; (C) 4%; (D) 6%; (E) 8% and (F) Pennisetin microparticles prepared in glacial acetic acid (MA).

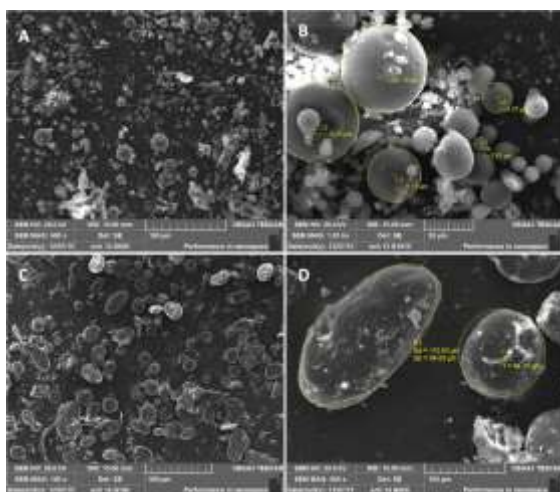


**Figure 2.** Scanning electron microscopy (SEM) images: (A-B) Pennisetin microparticles prepared in aqueous ethanol (ME) and (C-D) Pennisetin microparticles prepared in glacial acetic acid (MA).

The obtained pennisetin microparticles were compared to other prolamin microparticles, such as zein, kafirin and gliadin. In this study, ME and MA diameters were higher than those obtained using zein [16], kafirin [21] or gliadin [13], which were in the range of 0.1-0.26  $\mu\text{m}$ , 1-10  $\mu\text{m}$  and 0.15-0.25  $\mu\text{m}$ , respectively. Despite the similarity in amino acid sequence of pennisetin, kafirin and zein, the formulation of microparticles from these prolamins gave different particle sizes. This behavior may be attributed to their different hydrophobicity. Pennisetin was less hydrophobic and less cross linked than kafirin [8].

In this study, pennisetin microparticles seem to have the nearest characteristics to kafirin in term of particle shape. However, in term of particle size, pennisetin microparticles were larger than kafirin

ones. Taylor *et al.* [21] showed that low concentration of glacial acetic acid allowed producing kafirin microparticles with diameters ranging from 1 to 10  $\mu\text{m}$ . Whereas, MA were characterized by high diameters. This suggests that when using glacial acetic acid, the low pH may cause protein aggregation and denaturation [21]. Thus, it could be assumed that aqueous ethanol was more appropriate to form stable, homogeneous and spherical microparticles from pennisetin than glacial acetic acid using high speed and low antisolvent concentration.

### III.3. Scanning electron microscopy (SEM)

SEM images of the pennisetin microparticles are shown in Figure 2 (A-B) and (C-D) for ME and MA, respectively. As previously shown in OM images (Figure 1), MA appeared with light cracks and tough surface, they were characterized by spherical or irregular shape and high diameter varying from 20.56 to 168.83  $\mu\text{m}$  (Figure 2C-2D). By contrast, ME were regularly shaped relatively uniform in size with a smooth surface (Figure 2A-2B).

The ME diameters varied from 0.40 to 26.16  $\mu\text{m}$ . Zein and kafirin microparticles made by phase separation using aqueous ethanol exhibited comparable but smaller diameters as shown in previous works [20, 27]. This is probably due to the use of one form of zein the most abundant, which consists mainly of  $\alpha$ -zein. However, the pennisetin used in this study contained all the pennisetin subunits the 27, 22 and 12-kDa-pennisetins. It may be possible that the composition of the protein and the condition of preparation could influence microparticles morphology and size. In a previous work, Anyango *et al.* [28] showed that increasing amount of the cysteine-rich prolamin:  $\gamma$ -Kafirin conferred better stability to kafirin microparticles. In perspective, more work should be done, in preparation of pennisetin microparticles using separated subunit.

### III.4. Thermogravimetric analysis (TGA)

TGA were performed to study weight change as a function of temperature. TGA of pennisetin powder, ME and MA was carried out to compare their thermal stability. Figure 3A shows the weight loss curves of pennisetin powder and pennisetin microparticles from 20 to 450°C. Both MA and ME showed the same thermogravimetric profile with a slight difference, probably both compositions tend to degrade in a close manner.

However, it is possible to observe the existence of two steps as shown in Figure 3B representing the derived weight loss as a function of temperature

(DTG). The first step occurs below 100°C, probably corresponding to the elimination of both free and bound water, where the weight losses were 5.72, 5.73 and 4.83% for pennisetin powder, ME and MA, respectively. The first weight losses (Figure 3B) were respectively shown at 57°C for pennisetin powder and 60°C for both ME and MA. In the second step occurring between 100 and 450°C, more than 45.3% of pennisetin powder, 70% of ME and 65% of MA lose weight. This fact may probably correspond to covalent breaking of peptide bonds in amino acid residues. Comparable results were obtained by Liu and Ma [29] for wheat gluten, and Georget *et al.* [30] for kafirin. In the second step further heating causes a sudden decrease of weight accompanied with a sharp temperature peak of 308, 318 and 324°C for pennisetin powder, ME and MA, respectively (Figure 3A and 3B). Thus, ME and MA degraded at higher temperature than the native pennisetin, in the two steps, this is probably due to the increase of pennisetin cross linking during microparticle formation.

### III.5. Differential scanning calorimetry (DSC)

DSC is used to characterize the thermal and structural stability of pennisetin and the resulting microparticles during constant heat treatment. Thermal denaturation of a protein occurs at higher temperature. A protein is more stable, when, its thermal transition midpoint is high. DSC analysis results were shown in Figure 4 for pennisetin powder, ME and MA. Heat flow was recorded from 20 to 300°C. The endothermic peaks appeared at temperatures higher than 140°C and they reflected qualitatively the physical state changes in pennisetin powder, ME and MA. The most accentuated endothermic peaks were shown at 173.9 for ME, at 143.6°C for MA and at 159.1°C for pennisetin powder.

According to these results, ME appeared more heat stable than MA and the original pennisetin powder. The endothermic peaks might be related to different kind of bonds such as hydrogen bonding or Van der Waals forces. The corresponding denaturation enthalpy values increased during microparticles formation from 33.64 J/g for pennisetin powder to 38.90 and 43.69 J/g for ME and MA, respectively. Similar behavior was observed during casein microparticle formation, the coacervation process was associated with an increase in enthalpy corresponding to physical and chemical changes associated with protein aggregation [31, 32]. Consequently, it can be assumed that aqueous ethanol allowed to produce more heat stable microparticles than glacial acetic acid, the high enthalpy of MA is probably due to the protein aggregation as previously shown in Figure 1F. These endotherms may be due to the protein denaturation and  $\beta$ -sheet unfolding associated with

the remaining water and solvent removal. The zein DSC profile gave similar endothermic peaks but at lower temperature as previously described by Magoshi *et al.* [33].

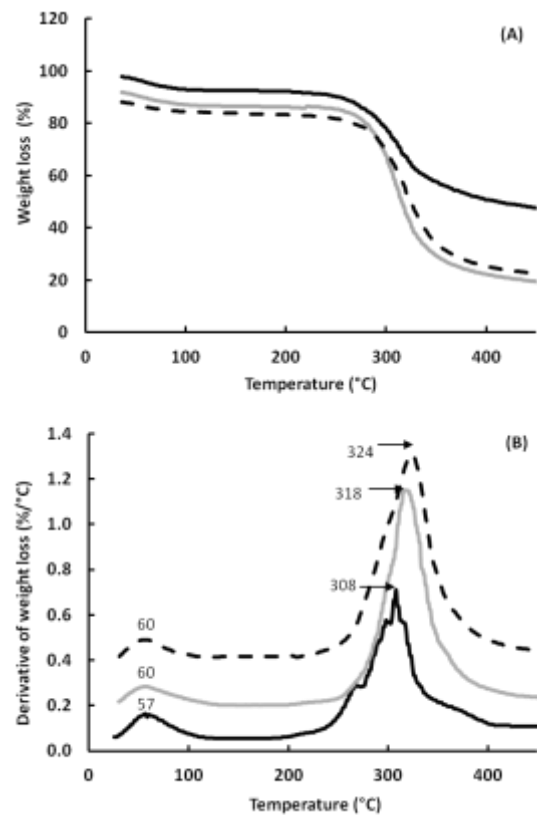


**Figure 3.** (A) Thermogravimetric Analysis (TGA) curves, (B) Derivative Thermogravimetric Analysis curves of (—) Pennisetin powder, (---) Pennisetin microparticles prepared in aqueous ethanol (ME), (.....) Pennisetin microparticles prepared in glacial acetic acid (MA).

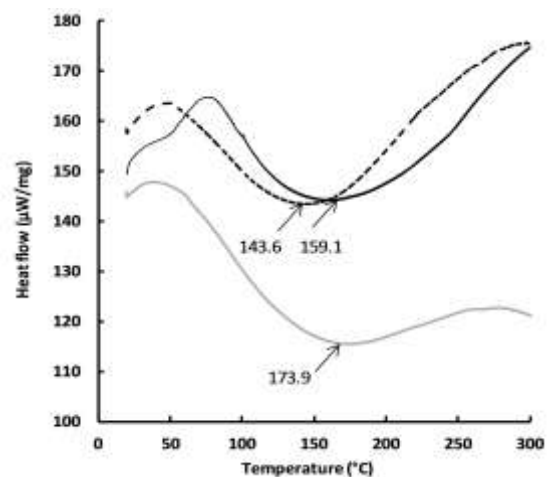


**Figure 4.** Differential scanning calorimetry (DSC) thermograms of (—) Pennisetin powder, (---) Pennisetin microparticles prepared in aqueous ethanol (ME), (.....) Pennisetin microparticles prepared in glacial acetic acid (MA).

### III.6. Fourier transform infrared spectroscopy (FTIR)

Experimental determination of the protein secondary structure by FTIR may provide important clues to the mechanism of microparticles formation by comparing the FTIR spectrum of pennisetin powder with the pennisetin microparticles ME and MA.

The normalized FTIR spectrum of pennisetin powder, ME and MA exhibited a similar profile with characteristic bands of protein bonds (Figure 5). The amide A appeared between 2800 and 3600  $\text{cm}^{-1}$  and corresponded to the stretching of the protein amino acids bonds N–H and O–H [21, 34]. The peptide groups amide I appeared at 1660 $\text{cm}^{-1}$  and was related to stretching of the amide groups carbonyl C=O [35]. The band at 1540  $\text{cm}^{-1}$  called amide II was related to the angular deformation vibrations of the N–H bond [9, 28].

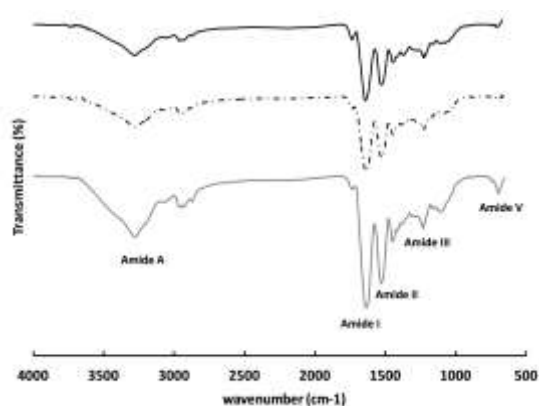


**Figure 5.** Fourier transform infrared spectroscopy (FTIR) spectra of (—) Pennisetin powder, (---) Pennisetin microparticles prepared in aqueous ethanol (ME), (.....) Pennisetin microparticles prepared in glacial acetic acid (MA).

The band at 1230  $\text{cm}^{-1}$  called amide III corresponded to the axial deformation vibrations of C–N bond [36]. The symmetrical stretching of C–O–C and the C–O stretching vibration appeared respectively at 1103 and 707 $\text{cm}^{-1}$ . The band at 700  $\text{cm}^{-1}$  was assigned to the amide V for  $\beta$ -form and random-coil [35].

As shown in table 2, the amides A, I, II, III increased in MA and ME compared to the initial pennisetin powder. Amides A and I obtained from the relative FTIR peak areas in pennisetin powder were 31.28 and 12.09%, respectively. However, in MA and ME, they increased yielding in MA 31.94 and 12.70% and much higher in ME 36.58 and 13.96%, respectively. In the meantime, Amide II, III and V were higher in MA (9.30, 7.45 and 1.40%) than ME (9.13, 4.67 and 0.50%).

**Table 2.** Percentage of Amide I, II, III, V and Amide A and secondary structure ratio.

	Pennisetin	ME	MA
<b>Amide I (%)</b>	12.09	13.96	12.70
<b>Amide II (%)</b>	8.22	9.13	9.30
<b>Amide III (%)</b>	4.07	4.67	7.45
<b>Amide V (%)</b>	0.56	1.40	0.50
<b>Amide A (%)</b>	31.28	36.58	31.94
<b>Amide I /Amide II</b>	1.47	1.53	1.37
<b><math>\alpha</math>-helix/<math>\beta</math>-sheet</b>	0.27	0.23	0.22

The changes of the secondary and tertiary structure of pennisetin and their microparticles were evaluated by the ratio Amide I /Amide II, this ratio was higher in ME (1.53) in comparison to MA (1.37) and pennisetin (1.47). Thus, secondary and tertiary structure of ME seemed to be more affected than MA and pennisetin. Amide I and Amide II are the most sensitive spectral regions typically used to predict protein secondary structure.

The second derivative of the FTIR spectra of amide I region was used to characterize and evaluate potential changes in secondary structure of pennisetin and microparticles (ME and MA). Four characteristic peaks resulted and were assigned to  $\alpha$ -helical structure at 1652  $\text{cm}^{-1}$ ,  $\beta$ -sheet at 1620 and 1691  $\text{cm}^{-1}$ ,  $\beta$ -turns at 1675  $\text{cm}^{-1}$  and random coil at 1648  $\text{cm}^{-1}$  [21]. As shown in figure 6, the predominant secondary structures were  $\beta$ -sheet and  $\beta$ -turn in all samples (pennisetin and its microparticles). The low level of  $\alpha$ -helical structure might be related to transition from native to aggregated protein mainly due to the high temperature of extraction and drying processes [37]. Bugs *et al.* [38] evaluated the secondary structure of pennisetin in the amide I region, they obtained much higher percentage of  $\alpha$ -helical structure (72%) and a lower percentage of  $\beta$ -sheet (9%) and  $\beta$ -turn (15%), this difference is probably due to the lower extraction temperature ( $-4^{\circ}\text{C}$ ) while in the present study the extraction procedure was carried out at  $60^{\circ}\text{C}$  where the percentage of  $\alpha$ -helical structure in pennisetin, ME and MA were 9.1, 11.56 and 9.38%, respectively.

The high proportion of  $\beta$ -sheet structure in ME compared to MA and initial pennisetin, could explain their thermal properties behavior thus ME were more stable than the initial pennisetin and MA. These results were in agreement with those obtained by DSC where ME appeared more heat stable ( $173.9^{\circ}\text{C}$ ) followed by pennisetin powder ( $159.1^{\circ}\text{C}$ ) and MA ( $143.6^{\circ}\text{C}$ ) (Figure 4). In the meantime the low percentage of  $\alpha$ -helical structure in pennisetin powder and microparticles could be

associated to a decrease in the native form, while the high percentage of  $\beta$ -sheet is generally related to protein aggregation [39]. The  $\alpha$ -helix/ $\beta$ -sheet ratio is used as indicator of protein structural change from native to aggregated [40]. In the present study this ratio was lower in ME and MA than pennisetin indicating that microparticles formation induced aggregation of the proteins. This high protein aggregation could be assumed to be responsible of the larger microparticle size obtained in MA and ME (Table 1) deeply related to  $\beta$ -sheet percentage of 50.64 and 43% for ME and MA, respectively (Figure 6).

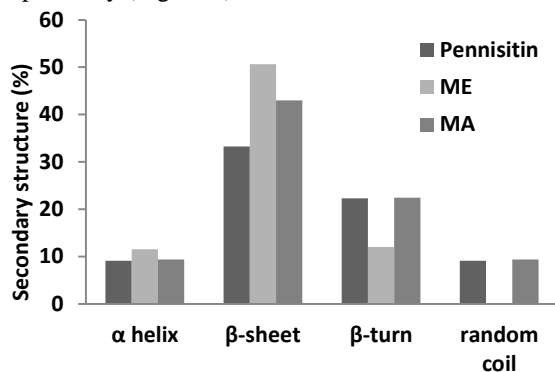


**Figure 6.** Percentage of secondary structure in the Amide I region based on FTIR analysis of pennisetin and pennisetin microparticles prepared in aqueous ethanol (ME), and pennisetin microparticles prepared in glacial acetic acid (MA).  $\alpha$ -Helix ( $1652\text{ cm}^{-1}$ ),  $\beta$ -Sheet ( $1620$  and  $1691\text{ cm}^{-1}$ ),  $\beta$ -Turn ( $1675\text{ cm}^{-1}$ ) and Random coil ( $1648\text{ cm}^{-1}$ ).

#### IV. Conclusion

In this paper, pennisetin microparticles were prepared by solvent phase separation. The effect of preparation process was investigated. Stable spherical microparticles were prepared using aqueous ethanol at lower antisolvent concentration and high mixing speed. Solvent type, antisolvent concentration and mixing speed had a highly significant effect ( $p < 0.001$ ) on microparticles diameters. SEM and OM images showed that MA were irregularly shaped and less stable than ME.

Thus, aqueous ethanol allowed forming spherical microparticles more regular and homogenous than those prepared with glacial acetic acid. Detailed analysis of SEM images showed that pennisetin microparticles surface was smooth, which presents an advantage to their application in food or drug encapsulation and delivery. The thermal and structural properties of pennisetin and its resulting microparticles were investigated by ATG and DSC ME were more heat stable than MA and the initial pennisetin.

The structural properties determined by FTIR, allowed the partial explanation of the microparticle formation. The percentage of Amide I, II, III, V and

Amide A increased in microparticles and in ME more than MA indicating formation of more covalent bond than the native protein. The predominant secondary structure was  $\beta$ -sheet in pennisetin powder, ME and MA, and was higher in ME and MA. This increase in  $\beta$ -sheet microparticle induced protein aggregation and microparticle formation. Pennisetin microparticles (ME and MA) as gluten free proteins might be good and safe ingredients for potential application in encapsulation of several bioactive products for vegans and celiac.

#### Acknowledgements

The Algerian ministry of scientific research is gratefully acknowledged for providing an Algerian CNEPRU grant numbered B00L01EN160220130001. Dr. Ousmaal Mohamed el Fadel from department of biology in Algiers University Benyoucef Benkhedda is knowledged for his assistance in OM and SEM image analysis.

#### V. References

- Sinha, V.R.; Trehan, A. Biodegradable microspheres for protein delivery. *Journal of Control Release* 90 (2003) 261-280.
- Nesterenko, A.; Alric, I.; Silvestre F.; Durrieu, V. Vegetable proteins in microencapsulation: A review of recent interventions and their effectiveness. *Industrial Crops and Products* 42 (2013) 469-479.
- Mehryar, L.; Esmaili, M.; Zeynali, F.; Sadeghi, R.; Imani, M. Evaluation of thermal stability of confectionary sunflower protein isolate and its effect on nanoparticulation and particle size of the produced nanoparticles. *Food Science and Biotechnology* 26 (2017) 653-662.
- Müller, V.; Piai, J.F.; Fajardo, A.R.; Fávoro, S.L.; Rubira, A.F.; Muniz, E.C. Preparation and characterization of zein and zein-chitosan microspheres with great prospective of application in controlled drug release. *Journal of Nanomaterials* (2011) 1-6.
- Liu, C.; Li, M.; Yang, J.; Xiong, L.; Sun, Q. Fabrication and characterization of biocompatible hybrid nanoparticles from spontaneous co-assembly of casein/gliadin and proanthocyanidin. *Food Hydrocolloids* 73 (2017) 74-89.
- Santos, M.B.; de Carvalho, C.W.P.; Garcia-Rojas E.E. Heteroprotein complex formation of bovine serum albumin and lysozyme: Structure and thermal stability. *Food Hydrocolloids* 74 (2018) 267-274.
- Gómez-Estaca, J.; Balaguer, M.P.; López-Carballo, G.; Gavara, R.; Hernández-Muñoz, P. Improving antioxidant and antimicrobial properties of curcumin by means of encapsulation in gelatin through electrohydrodynamic atomization. *Food Hydrocolloids* 70 (2017) 313-320.
- Bean, S.; Ioerger, B.P. Applied food protein chemistry in Sorghum and millet proteins. Ustunol Z (Ed). John Wiley and sons, Ltd. (2015). 323-359
- Forato, L.A.; Doriguetto, A.C.; Fischer, H.; Mascarenhas, Y.P.; Craievich, A.F.; Colnago, L.A. Conformation of the Z19 Prolamin by FTIR, NMR, and SAXS. *Journal of Agricultural and Food Chemistry* 52 (2004) 2382-2385.
- Marcellino, L.H.; Bloch, J.C.; Gander, E.S. Characterization of pearl millet prolamins. *Protein & Peptide Letters* 9 (2002) 237-244.
- Mauguet, M.C.; Legrand, J.; Brujes, L.; Carnelle, G.; Larre, C.; Popineau, Y. Gliadin matrices for microencapsulation processes by simple coacervation



- method. *Journal of Microencapsulation* 19 (2002) 377-384.
12. Patel, A.R.; Velikov, K.P. Zein as a source of functional colloidal nano- and microstructures. *Current Opinion in Colloid and Interface Science* 19 (2014) 450-458.
  13. Joye, J.J.; Nelis, V.A.; McClements, D.J. Gliadin-based nanoparticles: Fabrication and stability of food-grade colloidal delivery systems. *Food Hydrocolloids* 44 (2015) 86-93.
  14. Xue, F.; Li, C.; Liu, Y.; Zhu, X.; Pan, S.; Wang, L. Encapsulation of tomato oleoresin with zein prepared from corn gluten meal. *Journal of Food Engineering* 119 (2013) 439-445
  15. Park, C.E.; Park, D.J.; Kim, B.K. Effects of a chitosan coating on properties of retinol-encapsulated zein nanoparticles. *Food Science and Biotechnology* 24 (2015) 1725-1733.
  16. Parris, N.; Cooke, P.H.; Hicks, K.B. Encapsulation of essential oils in zein nanospherical particles. *Journal of Agricultural and Food Chemistry* 53 (2005) 4788-4792.
  17. Lau, E.T.L.; Giddings, S.J.; Mohammed, S.G.; Dubois, P.; Johnson, S.K.; Stanley, R.A.; Halley, P.J.; Steadman, K.J. Encapsulation of hydrocortisone and mesalazine in zein microparticles. *Pharmaceutics* 5 (2013) 277-293.
  18. Taylor, J.; Taylor, J.R.N.; Belton, P.S.; Minnaar, A. Kafirin microparticle encapsulation of catechin and sorghum condensed tannins. *Journal of Agricultural and Food Chemistry* 57 (2009b) 7523-7528.
  19. Links, M.R.; Taylor, J.; Kruger, M.C.; Naidoo, V.; Taylor, J.R.N. Kafirin microparticle encapsulated sorghum condensed tannins exhibit potential as an anti-hyperglycaemic agent in a small animal model. *Journal of Functional Foods* 20 (2016) 394-399.
  20. Lau, E.T.L.; Johnson, S.K.; Stanley, R.A.; Mereddy, R.; Mikkelsen, D.; Halley, P.J.; Steadman, K.J. Formulation and characterization of drug-loaded microparticles using distiller's dried grain kafirin. *Cereal Chemistry* 92 (2015) 246-252.
  21. Taylor, J.; Taylor, J.R.N.; Belton, P.S.; Minnaar, A. Formation of kafirin microparticles by phase separation from an organic acid and their characterisation. *Journal of Cereal Science* 50 (2009a) 99-105.
  22. Wang, L.; Gulati, P.; Santra, D.; Rose, D.; Zhang, Y. Nanoparticles prepared by proso millet protein as novel curcumin delivery system. *Food Chemistry* 240 (2018) 1039-1046.
  23. AOAC, (1995). Official Methods of Analysis, 16th ed. Method 46.30. Association of Official Analytical Chemists, Washington, USA.
  24. Gómez-Martínez, D.; Altskär, A.; Stading, M. Correlation between viscoelasticity, microstructure, and molecular properties of zein and pennisetin melts. *Journal of Applied Polymer Science* 125 (2012) 2245-2251.
  25. Kumar, P.; Lau, P.W.; Kale, S.; Johnson, S.; Pareek, V.; Utikar, R.; Lali, A. Kafirin adsorption on ion-exchange resins: Isotherm and kinetic studies. *Journal of Chromatography A* 1356 (2014) 105-116.
  26. R Core Team. R. A language and environment for statistical computing. R Foundation for Statistical Computing, Version R 4.0.2 URL <https://www.R-project.org/> (2020).
  27. Liu, X.; Sun, Q.; Wang, H.; Zhang, L.; Wang, J.Y. Microspheres of corn protein zein, for an ivermectin drug delivery system. *Biomaterials* 26 (2005) 109-115.
  28. Anyango, J.O.; Taylor, J.R.N.; Taylor, J. Role of  $\gamma$ -kafirin in the formation and organization of kafirin microstructures. *Journal of Agricultural and Food Chemistry* 61 (2013) 10757-10765.
  29. Liu, C.; Ma, X. Study on the mechanism of microwave modified wheat protein fiber to improve its mechanical properties. *Journal of Cereal Science* 70 (2016) 99-107.
  30. Georget, D.M.R.; Elkhalfifa, A.E.O.; Belton, P.S. Structural changes in kafirin extracted from a white type II tannin sorghum during germination. *Journal of Cereal Science* 55 (2012) 106-111.
  31. Saha, J.; Deka, S.C. Functional properties of sonicated and non-sonicated extracted leaf protein concentrate from *Diplazium esculentum*. *International Journal of Food Properties* 20 (2017) 1051-1061.
  32. Santinho, A.J.P.; Pereira, N.L.; De Freitas, O.; Collett, J.H. Influence of formulation on the physicochemical properties of casein microparticles. *International Journal of Pharmaceutics*. 186 (1999) 191-198.
  33. Magoshi, J.; Nakamura, S.; Murakami, K.I. Structure and physical properties of seed proteins I Glass transition and crystallization of zein protein from corn. *Journal of Applied Polymer Science*. 45 (1992) 2043-2048.
  34. Andreani, L.; Cerená, R.; Ramos, B.G.Z.; Soldi, V. Development and characterization of wheat gluten microspheres for use in a controlled release system. *Materials Science and Engineering C*. 29 (2009) 524-531.
  35. Pelton, J.T.; McLean, L.R. Spectroscopic methods for analysis of protein secondary structure. *Analytical Biochemistry* 277 (2000) 167-176.
  36. Jakobsen, R.J.; Brown, L.L.; Hutson, T.B.; Fink, D.J.; Veis, A. Intermolecular interactions in collagen self-assembly as revealed by Fourier transform infrared spectroscopy. *Science* 220 (1983) 1288-1290.
  37. Gao, Y.; Taylor, J.; Wellner, N.; Byaruhanga, Y.B.; Parker, M.L.; Mills, C.E.N.; Belton, P.S. Effect of preparation conditions on protein secondary structure and biofilm formation of kafirin. *Journal of Agricultural and Food Chemistry* 53 (2005) 306-312.
  38. Bugs, M. R.; Forato, L. A. ; Bortoleto-Bugs, R. K.; Fischer, H.; Mascarenhas, P. Y.; Ward, R. J.; Colnago, L. A. Spectroscopic characterization and structural modeling of prolamin from maize and pearl millet. *European Biophysics Journal* 33 (2004) 335-343.
  39. Wang, Y.; Tilley, M.; Bean, S.; Susan Sun, X.; Wang, D. Comparison of methods for extracting kafirin proteins from sorghum distillers dried grains with solubles. *Journal of Agricultural and Food Chemistry* 57 (2009) 8366-8372.
  40. Elkhalfifa, A.E.O.; Georget, D.M.R.; Barker, S.A.; Belton, P.S. Study of the physical properties of kafirin during the fabrication of tablets for pharmaceutical applications. *Journal of Cereal Science* 50 (2009) 159-165.

**Please cite this Article as:**

Bensalem A., Mosbahi S., Amoura A., Charabi A., Rogalski M., Magri P., Nadjemi B., Mokrane H., Factor affecting morphology, thermal and structural properties of pennisetin microparticles prepared by solvent phase separation. *Algerian J. Env. Sc. Technology*, 9:1 (2023) 2971-2979